IEEE Access
Multidisciplinary | Rapid Review | Open Access Journal

SPECIAL SECTION ON ENERGY HARVESTING TECHNOLOGIES FOR WEARABLE AND IMPLANTABLE DEVICES

Received July 25, 2020, accepted August 30, 2020, date of publication September 2, 2020, date of current version September 17, 2020.

Digital Object Identifier 10.1109/ACCESS.2020.3021230

A Highly Reliable SIMO Converter Using Hybrid Starter and Overcharging Protector for Energy Harvesting Systems

JAE-HYUNG JUNG, (Member, IEEE), SEONG-KWAN HONG, (Member, IEEE), AND OH-KYONG KWON, (Life Member, IEEE)

Department of Electronic Engineering, Hanyang University, Seoul 04763, South Korea

Corresponding author: Oh-Kyong Kwon (okwon@hanyang.ac.kr)

ABSTRACT This paper proposes a highly reliable single-inductor multi-output (SIMO) converter for energy harvesting systems, which is controlled by the power management controller (PMC) including the hybrid starter, overcharging protector (OCP), and switch controller (SWC). The proposed hybrid starter employs the power-on-reset to accurately control the activated and deactivated moments of the SWC, thus generating a system supply voltage (V_{SYS}) within the stable operating voltage range. The proposed OCP employs the diode-connection and Schmitt trigger schemes to monitor the voltage of a storage device (V_{STG}) in real time, thereby protecting the IC from being damaged without using either a capacitor or Zener diode, which causes the additional area or reverse leakage current, respectively. The proposed SIMO converter with the PMC was fabricated using 0.18-μm CMOS process. The measurement results show that V_{SYS} values at the activated and deactivated moments of the SWC are 1.798 V and 1.510 V, respectively, both of which are within the stable system voltage range for 1.8 V devices. In addition, the measured maximum V_{STG} is 5.892 V, which is much lower than an absolute maximum rated voltage of 9.2 V for 5 V devices. Furthermore, the measurement results reveal that the hybrid starter allows the proposed SIMO converter to be properly restarted immediately after V_{SYS} is shorted to ground, while the OCP safely protects the SIMO converter even when the storage device is removed from the IC while charging. Therefore, the proposed SIMO converter with the PMC is suitable for energy harvesting systems that require high reliability.

INDEX TERMS Energy harvesting, overcharging protection, SIMO converter, cold start, power-on-reset.

I. INTRODUCTION

The energy harvesting systems, which use harvesters as inputs to obtain various energies from the ambient environment, have become increasingly useful for Internet of Things (IoT) applications including wearable and implantable devices. The wearable devices use the ambient energy such as light [1], heat [2], and vibration [3] for easy access, whereas the implantable devices use the RF energy [4] for wireless power transfer. Both types of devices require a harvesting system with high reliability to prevent sudden damage caused by the accidental detachment of the storage device.

In the energy harvesting systems, the power converter is an essential block for the efficient and stable transfer of the energy from the input harvesters to the outputs with the storage device such as battery or supercapacitor [1], [5], [6].

Several power converters have been studied for energy harvesting systems to generate a stable system supply voltage from harvesters or storage devices [7]–[10]. However, they have often suffered from reliability problems caused by unstable supply voltage due to the harvested energy sensitive to the surroundings, or caused by insufficient protection for storage device due to the reverse leakage current.

The power converters in [7], [8] employ the start-up circuit and power-on-reset (POR) to provide a stable system supply voltage. In [7], the storage device itself is used as a system supply voltage, but its voltage range is limited to between 1 V and 1.8 V for safe operation of the power converter. A cold start circuit is employed in [8] to generate a system supply voltage, but its POR is heavily affected by the leakage current. The power converter in [9] employs a

The associate editor coordinating the review of this manuscript and approving it for publication was Abdul Halim Miah.

This work is licensed under a Creative Commons Attribution 4.0 License. For more information, see https://creativecommons.org/licenses/by/4.0/

battery management circuit to monitor the voltage state of the storage device by periodically comparing its resistor-divided voltage with a reference voltage, thus protecting the storage device from overcharging and undercharging. However, this converter can be suddenly damaged when the voltage of the storage device is abruptly increased to a value higher than the absolute maximum rated voltage during the periodic cycles for monitoring the storage device state. To protect from such damage, a capacitor with a capacitance value larger than 100 μF should be always placed at the storage device, leading to the additional area and cost. The power converter in [10] employs a Zener diode to prevent the voltage of the storage device from being increased over its turn-on voltage, but suffers from the reverse leakage current flowing through the Zener diode.

This paper proposes a highly reliable single-inductor multi-output (SIMO) converter for energy harvesting systems, which is controlled by the power management controller (PMC) including the hybrid starter, overcharging protector (OCP), and switch controller (SWC). The proposed hybrid starter employs the POR to accurately control the activated and deactivated moments of the SWC, thus producing a stable system supply voltage (V_{SYS}) within the stable operating voltage range. Furthermore, the proposed OCP monitors the voltage of the storage device in real time, thereby protecting the IC from being damaged without using a capacitor or Zener diode, which has conventionally been used. Section II describes the operating principle of the proposed SIMO converter with the PMC, and presents details on the implementation of the hybrid starter and OCP in the PMC. In Section III, the experimental results of the proposed SIMO converter with the PMC are analyzed and compared with those achieved in previous works. Finally, the conclusions are given in Section IV.

II. PROPOSED SIMO CONVERTER WITH PMC

A. OPERATING PRINCIPLE OF THE SIMO CONVERTER AND PMC

Fig. 1 shows the block diagram of the proposed SIMO converter with the PMC.

The proposed SIMO converter has two inputs (V_{STG} for the storage device and V_{HAR} for the harvester) and three outputs (V_{SYS} for the 1.8 V system supply voltage, V_{LOAD} for the 3.3 V output load, and V_{STG}). It also includes the input power switches (S_{I_STG} for the storage device and S_{I_HAR} for the harvester) and output power switches (S_{O_STG} for the storage device, S_{O_SYS} for V_{SYS}, and S_{O_LOAD} for V_{LOAD}). S_{EN} and S_{DN} are the switches to energize and de-energize the inductor (L) so as to increase and decrease the inductor current, respectively, for stable and efficient energy delivery. The above 7 switches are controlled by the switch control signals generated from the SWC in the PMC, thus determining the operation modes of the SIMO converter according to the combination of the inputs (V_{HAR} and V_{STG}) and outputs (V_{SYS}, V_{LOAD}, and V_{STG}). This ensures stable regulation of V_{SYS} and

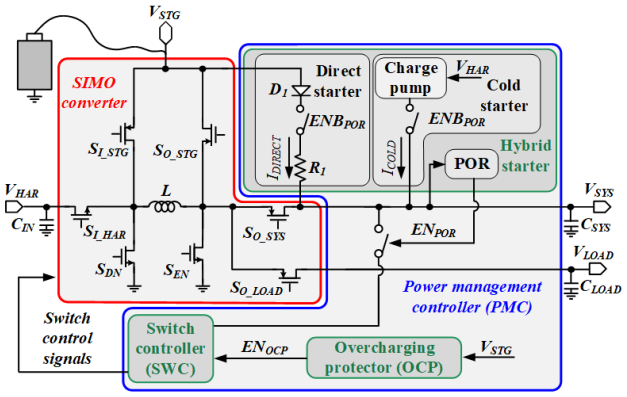

FIGURE 1. Block diagram of the proposed SIMO converter with the PMC.

TABLE 1. Design parameter specifications of the proposed SIMO converter.

Parameter	Description	Value
L	Inductor with a size of 7.2 mm x 7.2 mm x 4.8 mm (width x length x height)	22 µH (@ ESR: 61 mΩ)
C_{IN}	Input capacitor for harvester	4.7 µF
C_{SYS}	Output capacitor for V_{SYS}	22 µF
C_{LOAD}	Output capacitor for V_{LOAD}	22 µF

V_{LOAD} as well as efficient charging of V_{STG} by the buck-boost or boost operation [5]. Here, C_{IN} is an input capacitor, which is used as an input buffer for harvester, and C_{SYS} and C_{LOAD} are the output capacitors, which are respectively used for V_{SYS} and V_{LOAD} to ensure stable output regulation. In addition, all the parameter values used in this work are listed in Table 1. Moreover, unlike the previous works in [14]–[16] that employ the constant and adaptive on-time control methods, the proposed SWC employs the optimal on-time control method [5] that optimally adjusts the on-time by controlling the number of operation mode repetitions, thus improving the input and output regulation characteristics, peak output power, input and output voltage ranges, and power conversion efficiency.

The PMC includes the hybrid starter and OCP in addition to the aforementioned SWC. The hybrid starter, which consists of the direct starter, cold starter, and POR, produces a stable V_{SYS} during the start-up operation and maintains V_{SYS} within the stable operating range for the system. The OCP monitors the voltage of V_{STG} in real time to protect the SIMO converter from being damaged. The detailed implementations of the hybrid starter and OCP are described in the following Sections II. *B* and *C*, respectively.

B. HYBRID STARTER

Fig. 2 shows the timing diagram of the hybrid starter in Fig. 1. During the start-up operation in Fig. 2(a) and (b), the output of the POR (EN_{POR}) is initially low, and thus its inverted output

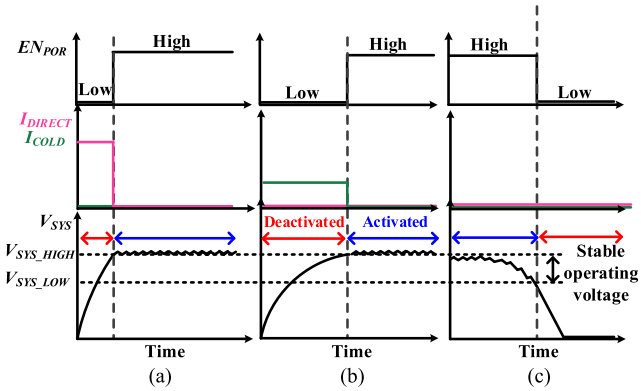

FIGURE 2. Timing diagrams of the hybrid starter using the POR: start-up and activated operation (a) using V_{STG} and (b) using V_{HAR}, and (c) deactivated operation.

(ENB_{POR}) enables either the direct starter to flow current through a diode (D_1) using V_{STG} (I_{DIRECT}) or the cold starter to flow current through a charge pump using V_{HAR} (I_{COLD}), thereby activating the SWC. The direct starter increases V_{SYS} to V_{SYS_HIGH} by providing I_{DIRECT} when V_{STG} is greater than or equal to $V_{SYS\_HIGH}+$ turn-on voltage of D_1 (V_{D1}), while preventing the inrush current through the use of R_1. Here, V_{SYS_HIGH} is the voltage of V_{SYS} that is high enough to activate the SWC. On the other hand, when V_{STG} is less than $V_{SYS\_HIGH} + V_{D1}$, the direct starter is unable to increase V_{SYS} to V_{SYS_HIGH}, and thus the cold starter provides I_{COLD} to increase V_{SYS} to V_{SYS_HIGH}. Since I_{COLD} is limited by the flying capacitor, operating frequency, and power switch sizes in the charge pump [13], the current level of I_{DIRECT} is higher than that of I_{COLD}. Consequently, the direct starter increases V_{SYS} to V_{SYS_HIGH} more quickly than the cold starter. When V_{SYS} reaches V_{SYS_HIGH}, EN_{POR} becomes high and both I_{DIRECT} and I_{COLD} stop flowing. As a result, V_{SYS} no longer increases while the SWC is activated, and thus the SIMO converter regulates V_{SYS} and V_{LOAD}, and charges V_{STG}. Once the SWC is activated, the POR in the hybrid starter continuously monitors the voltage level of V_{SYS}.

If no energy is supplied from V_{STG} or V_{HAR}, V_{SYS} decreases below V_{SYS_LOW}, which is outside the stable operating voltage range of the SWC, as shown in Fig. 2(c). Here, V_{SYS_LOW} is the voltage of V_{SYS} that is low enough to deactivate the SWC. At this moment, EN_{POR} becomes low, thus deactivating the SWC, and subsequently stopping the operation of the SIMO converter to avoid any malfunctions.

In this way, the direct starter or cold starter respectively produce I_{DIRECT} using V_{STG} or I_{COLD} using V_{HAR}, thus increasing V_{SYS} to V_{SYS_HIGH} in the start-up operation of the SIMO converter. The POR then controls the activated and deactivated operation of the SWC for stable operation of the SIMO converter.

Fig. 3(a) shows the schematic of the proposed POR, which consists of the POR core and self-reset level shifter (SRLS).

The POR core employs a bandgap reference structure, which includes bipolar transistors, *Q1* and *Q2*, resistors, *R3* and *R4*, current mirror using an active load with MOS transistors, M_1–M_6, and a common source amplifier with MOS transistors, M_7–M_{14}. In addition, the POR core employs a voltage divider including resistors, R_3–R_6, a MOS transistor, M_{15}, to provide hysteresis between V_{SYS_HIGH} and V_{SYS_LOW}, thereby preventing the SWC from repeating the activated and deactivated operations before settling to a stable state [11]. Moreover, to make the small-signal currents of Q_1 and Q_2 independent of the temperature, Q_1 and Q_2 are designed to have different base-emitter voltages considering the matching characteristics [12]. As such, the emitter area of Q_1 is designed to be 8 times larger than that of Q_2 in this work. Accordingly, the relationship between the transconductances of *Q1* (g_{m1}) and *Q2* (g_{m2}) can be given by $g_{m1} = 8g_{m2}$. As V_{SYS} reaches either of V_{SYS_HIGH} or V_{SYS_LOW}, the collector currents of Q_1 (I_{C1}) and Q_2 (I_{C2}) become the same, and EN_{POR} is inverted. Therefore, I_{C1} and I_{C2}, and the base

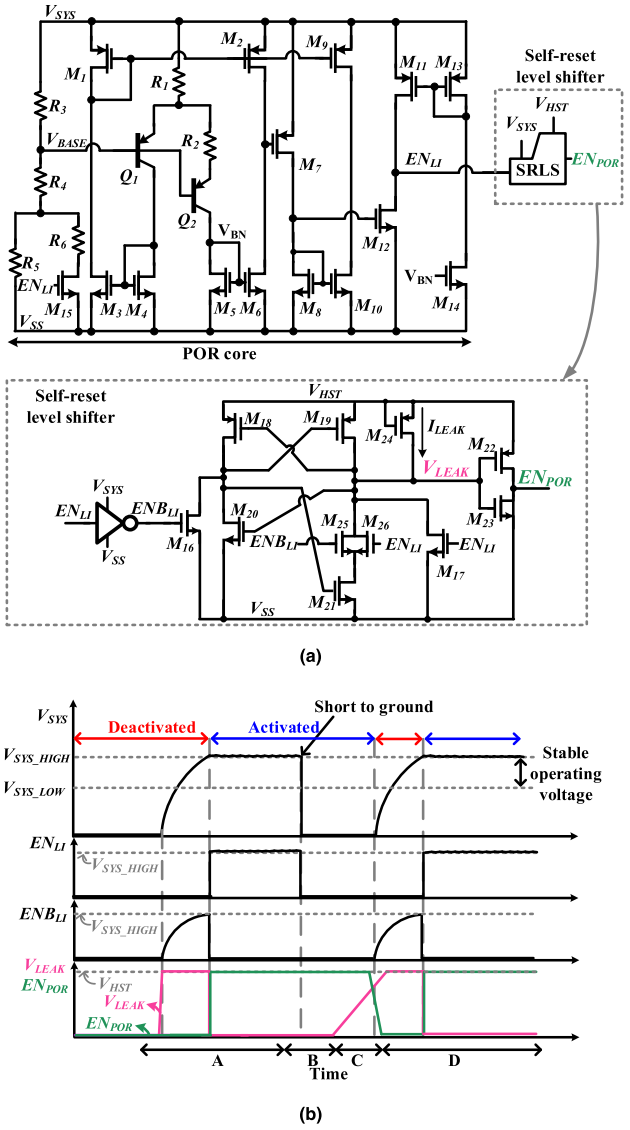

FIGURE 3. (a) Schematic and (b) timing diagram of the proposed POR.

voltage of Q_1 and Q_2 (V_{BASE}) can be expressed as

$$I_{C1} = I_{C2} = \frac{V_{BE2} - V_{BE1}}{R_2} = \frac{V_T \ln 8}{R_2}, \quad (1)$$

$$V_{BASE} = V_{SYS} - 2I_{C2}R_1 - V_{BE1} = V_{SYS} - 2\frac{R_1}{R_2}V_T \ln 8 - V_{BE1}, \quad (2)$$

where V_{BE1}, V_{BE2}, and V_T are the base-emitter voltages of Q_1 and Q_2, and the thermal voltage, respectively. Since V_{BE1} and V_{BE2} have a negative temperature coefficient and V_T has a positive temperature coefficient, V_{BASE} has a constant value even when the temperature varies. Consequently, V_{SYS_HIGH} and V_{SYS_LOW} have the constant values, which are independent of the process and temperature, and can be expressed as

$$V_{SYS\_HIGH} = \frac{R_4+(R_5||R_6)}{R_3+R_4+(R_5||R_6)} \cdot V_{BASE}(WhenEN_{LI} = V_{SYS}), \quad (3)$$

$$V_{SYS\_LOW} = \frac{R_4+R_5}{R_3+R_4+R_5} \cdot V_{BASE}(WhenEN_{LI} = 0). \quad (4)$$

In this way, the POR core ensures that V_{SYS} is within the stable operating range for the SWC, which is between V_{SYS_HIGH} and V_{SYS_LOW}, both of which are independent of process and temperature.

The SRLS, which shifts the supply voltage level from V_{SYS} to V_{HST}, is implemented to enable the restart of the proposed SIMO converter even when V_{SYS} is suddenly shorted to ground, where V_{HST} is the highest voltage among V_{HAR}, V_{STG}, V_{SYS}, and V_{LOAD}. The SRLS employs the conventional level shifter with MOS transistors, M_{16}–M_{23}, while including the additional MOS transistors, M_{24}–M_{26}, which are used to reset the gate voltage of M_{22} and M_{23} (V_{LEAK}) when V_{SYS} is shorted to ground. Here, M_{25}–M_{26} are used to completely disconnect V_{LEAK} from ground, while M_{24} allows leakage current (I_{LEAK}) to flow into V_{LEAK}, thus resetting EN_{POR} to low.

Fig. 3(b) shows the timing diagram of the proposed POR. In the start-up and activated operation (period A), the direct starter using V_{STG} or the cold starter using V_{HAR} increases V_{SYS} to V_{SYS_HIGH}, and then EN_{LI}, ENB_{LI}, EN_{POR}, and V_{LEAK} become high (V_{SYS}), low (0 V), high (V_{HST}), and 0 V, respectively, thus activating the SWC. Here, EN_{LI} and ENB_{LI} are the output of the POR core and its inverted output, respectively. When V_{SYS} is suddenly shorted to ground (period B), both EN_{LI} and ENB_{LI} become low (0 V), and EN_{POR} remains high (V_{HST}). Even though EN_{POR} is high (V_{HST}), the SWC is unable to operate because V_{SYS} is 0 V, which is outside the stable operating voltage range. As the leakage current of M_{24} gradually increases V_{LEAK} to V_{HST} (period C), EN_{POR} is reset to low (0 V), and then the hybrid starter increases V_{SYS} to V_{SYS_HIGH} (period D). Consequently, EN_{LI}, ENB_{LI}, EN_{POR}, and V_{LEAK} become high (V_{SYS}), low (0 V), high (V_{HST}), and 0 V, respectively, thus activating the SWC to restart the SIMO converter. In this way, the POR enables the hybrid converter to accurately activate and deactivate the SWC for stable V_{SYS} between V_{SYS_HIGH} and V_{SYS_LOW}, while the SRLS resets

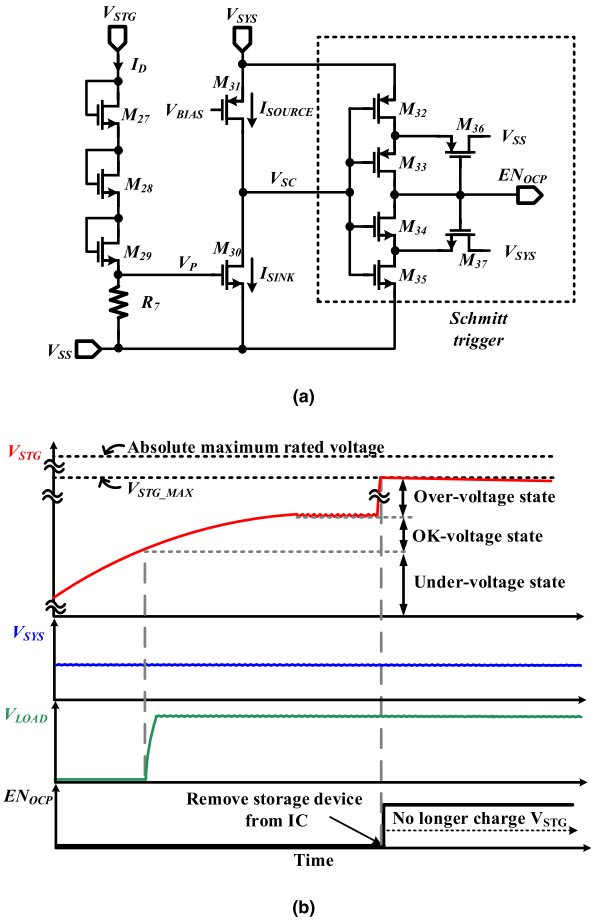

FIGURE 4. (a) Schematic and (b) timing diagram of the proposed OCP.

EN_{POR} to restart the proposed SIMO converter even when V_{SYS} is suddenly shorted to ground.

C. OVERCHARGING PROTECTOR

Fig. 4(a) shows the schematic of the proposed OCP that employs the diode-connection and Schmitt trigger schemes to monitor the voltage of V_{STG} in real time. The proposed OCP includes the diode-connected MOS transistors, M_{27}–M_{29}, current-to-gate voltage generator with resistor, R_7, sinking bias MOS transistor, M_{30}, sourcing bias MOS transistor, M_{31}, and Schmitt trigger with MOS transistors, M_{32}–M_{37}. As V_{STG} increases to a value high enough to turn on M_{27}–M_{29}, the sink and source currents (I_{SINK} and I_{SOURCE}) respectively flow through M_{30} and M_{31}, which can be expressed as

$$I_{SINK} = \frac{1}{2}\frac{W}{L}\mu_n C_{OX}(V_P - V_{THN})^2, \quad (5)$$

$$I_{SOURCE} = \frac{1}{2}\frac{W}{L}\mu_P C_{OX}(|V_{SYS} - V_{BIAS} - V_{THP}|)^2, \quad (6)$$

where V_{BIAS}, C_{OX}, μ_n, μ_p, V_{THN}, and V_{THP} are the reference bias voltage generated from the bandgap reference generator, oxide capacitance, and the mobility and threshold voltages of the NMOS and PMOS transistors, respectively. When V_{STG} increases to a value near its maximum operating

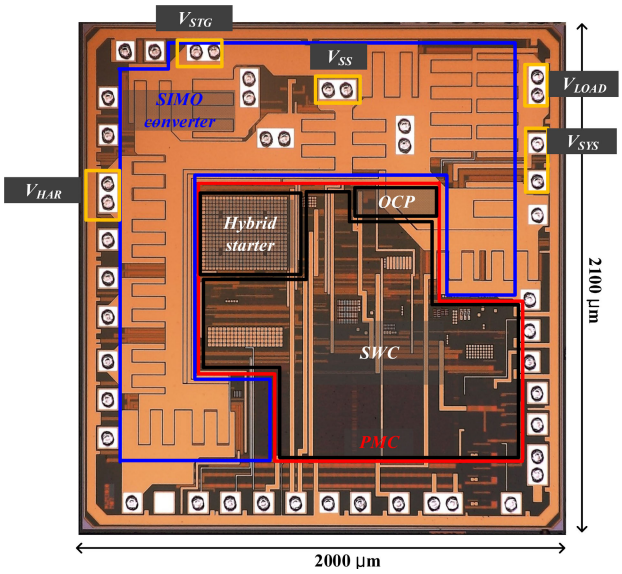

FIGURE 5. Chip photomicrograph of the proposed SIMO converter with the PMC.

voltage (V_{STG_MAX}), which is lower than the absolute maximum rated voltage, the input voltage of the Schmitt trigger (V_{SC}) increases to its logic threshold voltage according to the above I_{SOURCE} and I_{SINK}, and the OCP produces its output (EN_{OCP}) high, thus no longer charging V_{STG}.

Fig. 4(b) shows the timing diagram of the proposed OCP. As V_{STG} begins to be charged, the PMC periodically monitors the V_{STG} state, which is determined as the under-voltage state, OK-voltage state, or over-voltage state by comparing V_{STG} with a pre-fixed reference voltage [9]. In the under-voltage state, V_{HAR} charges V_{STG} and regulates V_{SYS} without regulating V_{LOAD}. In the OK-voltage state, V_{HAR} and V_{STG} regulate both V_{SYS} and V_{LOAD}, while the surplus energy in V_{HAR} is used to charge V_{STG}. In the over-voltage state, V_{HAR} and V_{STG} regulate both V_{SYS} and V_{LOAD} as in the OK-voltage state, but the surplus energy in V_{HAR} is no longer used to charge V_{STG}. Even when V_{STG} abruptly increases to V_{STG_MAX} due to the sudden removal of a storage device from the IC while charging, the proposed OCP produces EN_{OCP} high and makes the SWC no longer charge V_{STG}. In this way, the proposed OCP protects the SIMO converter from being damaged without using a capacitor or Zener diode, which causes the additional area or reverse leakage current, respectively.

III. EXPERIMENTAL RESULTS

Fig. 5 shows a chip photomicrograph of the proposed SIMO converter with the PMC, which was fabricated using 0.18-μm standard CMOS process technology.

Fig. 6 shows the measurement environment for testing the proposed hybrid starter and OCP. It consists of an oscilloscope (LeCroy 104MXi), evaluation board, storage device (Li-ion battery (BAK LP-402025-IS-3) or supercapacitor (TDK EDLC252520-351-2F-21)), photovoltaic cell (IXYS KXOB22-04 × 3F), and lamp. The fabricated IC is packaged

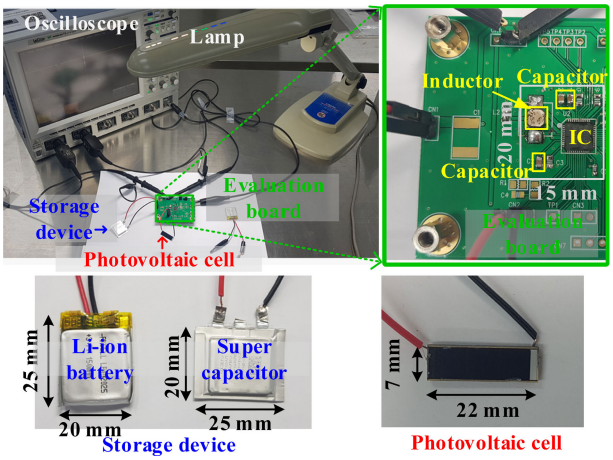

FIGURE 6. Measurement environment.

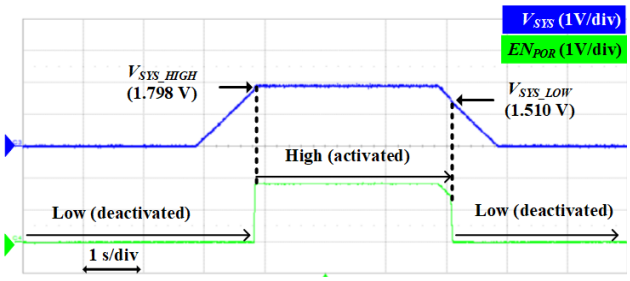

FIGURE 7. Measured EN_{POR} when V_{SYS} increases to V_{SYS_HIGH} and decreases to ground.

using quad-flat no-leads (QFN) with a size of 6 mm × 6 mm and attached to the evaluation board. The active area of the evaluation board including the fabricated IC and passive devices (capacitor and inductor) is 15 mm × 20 mm. The storage device is used with either Li-ion battery or supercapacitor. The capacity and size of the Li-ion battery are 165 mAh and 20 mm × 25 mm, respectively. The capacitance value and size of the supercapacitor are 350 mF and 25 mm × 20 mm, respectively. The photovoltaic cell is used as an input harvester and its size is 22 mm × 7 mm. In addition, the lamp is used to control the brightness of the photovoltaic cell.

Fig. 7 shows the measured EN_{POR} when V_{SYS} increases to V_{SYS_HIGH} and decreases to ground, showing that the SWC is properly activated and deactivated as EN_{POR} becomes high at a V_{SYS} of 1.798 V and low at a V_{SYS} of 1.510 V, respectively, for stable operation of the SIMO converter.

Fig. 8(a) and (b) show the measurement results of the SIMO converter without and with the SRLS, respectively, at a V_{STG} of 4 V, when V_{SYS} is shorted to ground. The direct starter using V_{STG} increases V_{SYS} to V_{SYS_HIGH}, thus activating the SWC in the start-up operation, and then enables the SIMO converter to properly regulate V_{SYS} and V_{LOAD} regardless of the SRLS. However, after V_{SYS} is shorted to ground, the proposed SIMO converter without the SRLS cannot be restarted

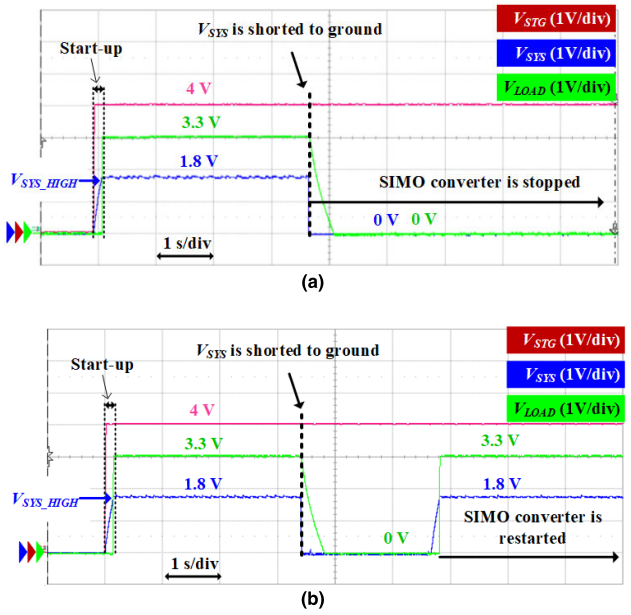

FIGURE 8. Measurement results of the SIMO converter (a) without and (b) with SRLS at a V_{STG} of 4 V when V_{SYS} is shorted to ground.

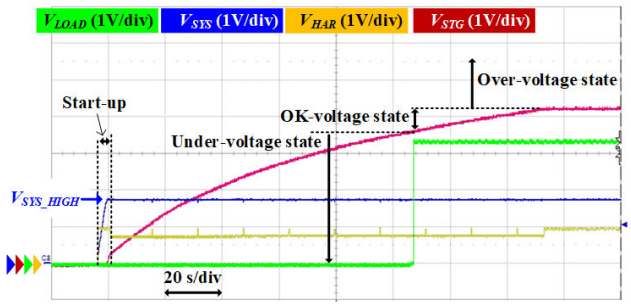

FIGURE 9. Measurement result of the SIMO converter for start-up operation using the harvester at the initial V_{STG} and V_{HAR} of 0 V and 1 V, respectively.

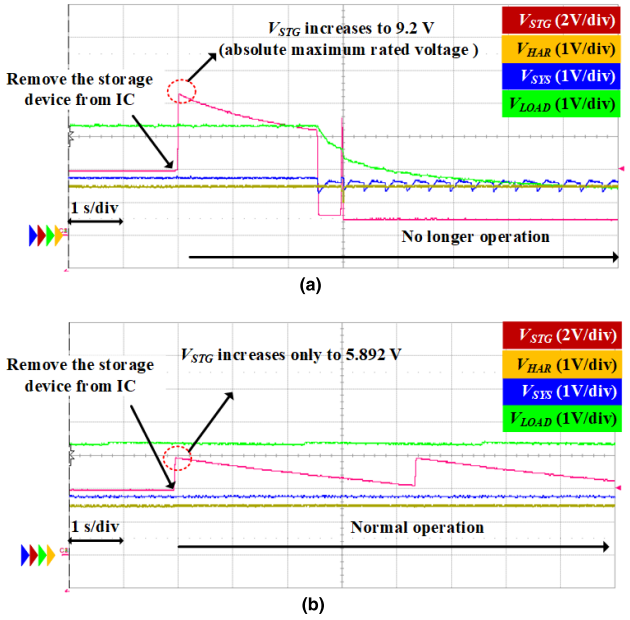

FIGURE 10. Measurement results of the SIMO converter (a) without and (b) with the proposed OCP when the storage device is removed from the IC while charging.

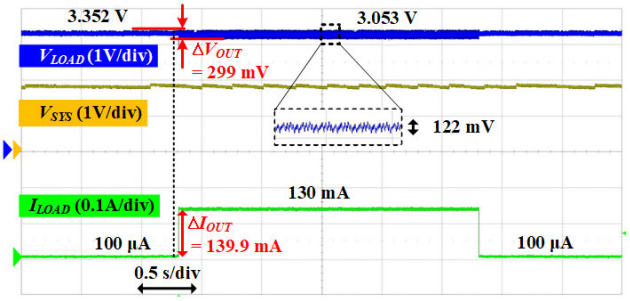

FIGURE 11. Measured output voltage at V_{LOAD} when the load current varies from 100 μA to 130 mA and vice versa.

as shown in Fig. 8(a) because it is unable to reset the output of the POR. On the other hand, the SIMO converter with the SRLS can be properly restarted, while regulating V_{SYS} and V_{LOAD} as shown in Fig. 8(b), demonstrating that the proposed POR with the SRLS properly works for stable restart and regulation.

Fig. 9 shows the measurement result of the SIMO converter when a V_{HAR} of only 1 V is initially applied, while V_{STG} is set to 0 V, showing that the cold starter using V_{HAR} properly performs the start-up operation, thus enabling the SIMO converter to operate according to the V_{STG} state.

Fig. 10(a) and (b) show the measurement results of the SIMO converter without and with the proposed OCP, respectively, when the storage device is removed from the IC while charging. When the storage device is connected to the IC, the proposed SIMO converter charges V_{STG} and regulates V_{SYS} and V_{STG} regardless of the OCP. However, after the storage device is suddenly removed from IC, the proposed SIMO converter without the proposed OCP no longer operates due to the damage caused as V_{STG} abruptly increases to a value higher than an absolute maximum rated voltage of 9.2 V. On the other hand, the SIMO converter with the OCP increases V_{STG} only to 5.892 V, which is much lower than an absolute maximum rated voltage of 9.2 V for 5 V devices, thus properly charging V_{STG}, and regulating V_{SYS} and V_{LOAD}, demonstrating that the proposed OCP safely protects the IC without using an additional capacitor or Zener diode, which has been used in the conventional SIMO converter.

Fig. 11 shows the measured output voltage at V_{LOAD} when the load current varies from 100 μA to 130 mA and vice versa. The measurement result shows that a ripple voltage of 122 mV was measured at V_{LOAD} as the load current (I_{LOAD}) varied from 100 μA to 130 mA and vice versa, and subsequently the load regulation was calculated to be only 2.3 mV/mA, which was obtained by dividing a ΔV_{OUT} of 299 mV by a ΔI_{OUT} of 139.9 mA, demonstrating that the proposed converter properly regulates V_{LOAD} even when I_{LOAD} varies. Here, ΔI_{OUT} is the change in I_{LOAD}, and ΔV_{OUT} is the change in voltage at V_{LOAD}.

TABLE 2. Performance comparison with previous works.

	This work	[9]	[10]	[14]	[15]	[16]
Process (μm)	0.18	0.35	Use discrete IC	0.18	0.18	0.5
System supply voltage	Output of the SIMO converter	Storage device	Storage device	Output of SIMO converter	Output of the SIMO converter	Output of the SIMO converter
Restart function when system voltage is shorted	Yes	No	No	No	No	No
Overcharging protection function for storage device	Yes	Yes	Yes	No	No	No
Additional devices required for overcharging protection	No	Yes (Capacitor over than 100 μF)	Yes (Zener diode)	-	-	-
Static current consumed for overcharging protection	55 nA ($@V_{STG}$: 4 V)	N/A	600 nA ($@V_{STG}$:4 V)	-	-	-
Peak output power	462 mW	N/A	N/A	2.5 mW	10 mW	13 mW
Output voltage	1.8 V & 3.3 V (regulated)	Max. 5 V (not regulated)	N/A	1.8 V (regulated)	1.0 V & 1.8 V (regulated)	1 V ~ 3.3 V (regulated)
Peak power efficiency	89.2%	93.0% *	N/A	83.0 %	83.0%	90.0%

N/A : not applicable
* Requires an additional DC-DC converter to regulate the output voltage, resulting in a decrease in total power efficiency.

TABLE 1 shows the functional comparison of the proposed SIMO converter with previous works. Compared to other works, only the proposed work has both the restart function when the system voltage is shorted to ground and the protection function when the storage device is suddenly removed. In addition, the proposed SIMO converter outperformed previous works in most performances including the peak output power and peak power efficiency. The works in [9] and [16] achieved a slightly higher power efficiency than the proposed converter, but the former [9] required an additional DC-DC converter to regulate the output voltage, resulting in an increase in chip area and a decrease in total power efficiency, and the latter [16] suffered from a very low peak output power of 13 mW, which is only applicable for indoor energy harvesting IoT applications.

IV. CONCLUSION

This paper proposes a highly reliable SIMO converter for energy harvesting systems, which is controlled by the PMC including the hybrid starter, OCP, and SWC. The proposed hybrid starter employs the POR to generate V_{SYS} by accurately controlling the activated and deactivated moments of the SWC, thus ensuring that V_{SYS} is within the stable operating voltage range. The proposed OCP monitors V_{STG} in real time, thus protecting the IC from being damaged without using the capacitor or Zener diode, which causes the additional area or reverse leakage current, respectively. The measurement results showed that V_{SYS} values at the activated and deactivated moments of the SWC were 1.798 V and 1.510 V, respectively, both of which were within the stable system voltage range for 1.8 V devices. In addition, the measured maximum V_{STG} was 5.892 V, which was much lower than an absolute maximum rated voltage of 9.2 V for 5 V devices. Furthermore, the measurement results revealed that the hybrid starter properly restarted the proposed SIMO converter immediately after V_{SYS} was shorted to ground, while the OCP safely protected the SIMO converter even when the storage device was removed from the IC while charging. Therefore, the proposed SIMO converter with the PMC is suitable for energy harvesting systems requiring high reliability.

REFERENCES

[1] P.-H. Chen, C. Shiang, and K.-C. Lin, "A 50 nW-to10 mW output power tri-mode digital buck converter with self-tracking zero current detection for photovoltaic energy harvesting," *IEEE J. Solid-State Circuits*, vol. 51, no. 2, pp. 523–532, Feb. 2016.

[2] Y. K. Ramadass and A. P. Chandrakasan, "A batteryless thermoelectric energy-harvesting interface circuit with 35 mV startup voltage," *IEEE J. Solid-State Circuits*, vol. 46, no. 1, pp. 333–341, Jan. 2011.

[3] D. Kwon and G. A. Rincon-Mora, "A single-inductor 0.35 μm CMOS energy-investing piezoelectric harvester," *IEEE J. Solid-State Circuits*, vol. 49, no. 10, pp. 2277–2291, Oct. 2014.

[4] H. Jabbar, Y. Song, and T. Jeong, "RF energy harvesting system and circuits for charging of mobile devices," *IEEE Trans. Consum. Electron.*, vol. 56, no. 1, pp. 247–253, Feb. 2010.

[5] J.-H. Jung, Y.-H. Jung, S.-K. Hong, and O.-K. Kwon, "A high peak output power and high power conversion efficiency SIMIMO converter using optimal on-time control and hybrid zero current switching for energy harvesting systems in IoT applications," *IEEE Trans. Power Electron.*, vol. 35, no. 8, pp. 8261–8275, Aug. 2020.

[6] N.-M. Sze, F. Su, Y.-H. Lam, W.-H. Ki, and C.-Y. Tsui, "Integrated single-inductor dual-input dual-output boost converter for energy harvesting applications," in *Proc. IEEE Int. Symp. Circuits Syst.*, May 2008, pp. 2218–2221.

[7] S. S. Amin and P. P. Mercier, "MISIMO: A multi-input single-inductor multi-output energy harvesting platform in 28-nm FDSOI for powering net-zero-energy systems," *IEEE J. Solid-State Circuits*, vol. 53, no. 12, pp. 3407–3419, Dec. 2018.

[8] P.-H. Chen, K. Ishida, K. Ikeuchi, X. Zhang, K. Honda, Y. Okuma, Y. Ryu, M. Takamiya, and T. Sakurai, "Startup techniques for 95 mV step-up converter by capacitor pass-on scheme and V_{TH}-tuned oscillator with fixed charge programming," *IEEE J. Solid-State Circuits*, vol. 47, no. 5, pp. 1252–1260, May 2012.

[9] Texas Instruments. *bq25570—Ultra Low-Power Boost Converter With Battery Management for Energy Harvester Applications Datasheet*. Accessed: Mar. 2019. [Online]. Available: http://www.ti.com/product/BQ25570

[10] D. Carli, D. Brunelli, L. Benini, and M. Ruggeri, "An effective multi-source energy harvester for low power applications," in *Proc. Design, Automat. Test Eur.*, Grenoble, France, Mar. 2011, pp. 1–6.
[11] Texas Instruments. *SLVA769A—Understanding Undervoltage Lockout in Power Devices*. Accessed: Sep. 2018. [Online]. Available: https://www.ti.com/lit/an/slva769a/slva769a.pdf
[12] R. J. Baker, H. W. Li, and D. E. Boyce, *CMOS: Circuit Design, Layout, and Simulation*. Piscataway, NJ, USA: IEEE Press, 1998.
[13] Y. K. Ramadass and A. P. Chandrakasan, "Voltage scalable switched capacitor DC–DC converter for ultra-low-power on-chip applications," in *Proc. IEEE Power Electron. Spec. Conf.*, Orlando, FL, USA, Jun. 2007, pp. 2353–2359.
[14] S. Bandyopadhyay and A. P. Chandrakasan, "Platform architecture for solar, thermal, and vibration energy combining with MPPT and single inductor," *IEEE J. Solid-State Circuits*, vol. 47, no. 9, pp. 2199–2215, Sep. 2012.
[15] G. Yu, K. W. R. Chew, Z. C. Sun, H. Tang, and L. Siek, "A 400 nW single-inductor dual-input–tri-output DC–DC buck–boost converter with maximum power point tracking for indoor photovoltaic energy harvesting," *IEEE J. Solid-State Circuits*, vol. 50, no. 11, pp. 2758–2772, Nov. 2015.
[16] P.-C. Huang and T.-H. Kuo, "A reconfigurable and extendable single-inductor single-path three-switch converter for indoor photovoltaic energy harvesting," *IEEE J. Solid-State Circuits*, vol. 55, no. 7, pp. 1998–2008, Jul. 2020.

JAE-HYUNG JUNG (Member, IEEE) received the B.S. degree in electronics and computer engineering from Hanyang University, Seoul, South Korea, in 2012, where he is currently pursuing the Ph.D. degree in electronics and computer engineering. His research interests include power management IC design for energy harvesting, battery charger, and low dropout regulator.

SEONG-KWAN HONG (Member, IEEE) received the B.S. degree in electronic engineering from Hanyang University, Seoul, South Korea, in 1980, and the M.S. and Ph.D. degrees in electrical engineering from the Georgia Institute of Technology, Atlanta, GA, USA, in 1985 and 1994, respectively.

From 1990 to 1995, he was with Cadence Design Systems Inc., San Jose, CA, USA, where he developed several ECAD products. In 1995, he joined the Research and Development Laboratory, LG Semicon Company Ltd., Seoul, where he was in charge of Design Technology Center as a Research Fellow. In 1999, he became a Vice President and a Chief Information Officer at Hynix Semiconductor Inc., where he was responsible for the Information Technology and Research and Development Engineering support. From 2009 to 2013, he was with Yonsei University, Seoul, as a Hynix Chair and a Research Professor. In 2013, he joined Hanyang University as a Research Professor. His research interests include EDA design methodology, mixed IC design, and automotive IC design.

OH-KYONG KWON (Life Member, IEEE) received the B.S. degree in electronic engineering from Hanyang University, Seoul, South Korea, in 1978, and the M.S. and Ph.D. degrees in electrical engineering from Stanford University, Stanford, CA, USA, in 1986 and 1988, respectively. From 1987 to 1992, he was with the Semiconductor Process and Design Center, Texas Instruments Inc., Dallas, TX, USA, where he was involved in the development of multichip module technologies and smart power integrated circuit technologies for automotive and flat panel display applications. In 1992, he joined Hanyang University as an Assistant Professor at the Department of Electronic Engineering. He is currently a Professor with the Department of Electronic Engineering, Hanyang University. He has authored and coauthored over 313 international journal and conference papers and 224 U.S. patents. His research interests include interconnect and electrical noise modeling for high-speed system-level integration, wafer-scale chip-size packages, smart power integrated circuit technologies, mixed mode signal circuit design, imager, analog front-end circuit design for bio-medical instruments, and the driving methods and circuits for flat panel displays.